Polymeric Monolayer Dynamics at the Air/Water Interface by Surface Light Scattering

Masami Kawaguchi,† Bryan B. Sauer,‡ and Hyuk Yu*

Department of Chemistry, University of Wisconsin, Madison, Wisconsin 53706.
Received April 8, 1988

ABSTRACT: The static and dynamic properties of six different polymer monolayers at the air/water interface were examined with the surface quasi-elastic light scattering technique combined with the static Wilhelmy plate method. The polymers studied in order of increasing hydrophobicity were poly(ethylene oxide) (PEO), polytetrahydrofuran (PTHF), poly(vinyl acetate) (PVAc), poly(methyl acrylate) (PMA), poly(methyl methacrylate) (PMMA), and poly(*tert*-butyl methacrylate) (PtBMA). The isotherms of surface pressure versus surface area per unit mass can be classified into two types: PEO, PTHF, PVAc, and PMA exhibit the behavior of expanded-type monolayers and PMMA and PtBMA show that of condensed-type monolayers. The spectral data were analyzed in terms of the dispersion equation for capillary wave motion, and the dynamic longitudinal elasticity ϵ and the corresponding viscosity κ of the monolayers as a function of surface concentration were deduced. The static and dynamic elasticities were found to be the same over a majority of the concentration range. For the expanded-type monolayers, ϵ predominates over κ in determining the overall dynamic modulus ϵ^*. For the condensed monolayers, PMMA and PtBMA, on the other hand, ϵ and κ contribute about equally to ϵ^*. The absolute magnitudes of ϵ and κ increased with increasing hydrophobicity, with PEO the least and PtBMA the greatest.

Introduction

Polymers of varying hydrophobicity are well-known to form expanded- and condensed-type monolayers. The reasons for this classification have been proposed to be rather complicated.[1,2] The nature of the monolayer partially depends on the strength of interfacial interactions with substrate molecules and that of polymer intersegmental interactions. We therefore expect that the viscoelastic properties of polymer monolayers are also dependent on these factors. It seems most desirable then to perform a systematic study of polymer monolayers to examine their viscoelasticity by means of the surface light scattering (SLS) technique. SLS probes surface capillary waves, spontaneously induced by thermal fluctuations in the underlying liquids, and its uniqueness lies in the fact that no contact with the interface is needed through any sort of mechanical means. The power spectra obtained from the capillary wave scattering are fitted to a Lorentzian profile giving the frequency shift f_s (peak frequency), corresponding to the propagation velocity of the waves, and the corrected spectral width $\Delta f_{s,c}$, corresponding to a temporal damping of the waves. The values of $\Delta f_{s,c}$ were predicted to undergo a maximum at intermediate surface longitudinal elasticities first by Dorrestein,[3] and later Lucassen and Hansen[4,5] verified experimentally that a damping maximum occurs. This damping maximum is caused by resonant mode couplings between the transverse capillary waves and the longitudinal waves which are governed by the longitudinal elasticity ϵ and corresponding viscosity κ. Only the transverse waves contribute to the scattering intensity[6] but the mode couplings allow one to deduce ϵ and κ from the power spectra of quasi-elastically scattered light. The resonance occurs at an intermediate elasticity; the value of the longitudinal elasticity ϵ where the maximum occurs is about 13 dyn/cm at the air/water interface (A/W).[7] Hence, the method has a severe limitation in the accessible range of elasticities. If ϵ is greater than about 40 dyn/cm, the wave motion becomes insensitive to any change in ϵ, and thus ϵ and κ can no longer be deduced.

The most common systems studied with wave damping techniques in the past were small-molecule amphiphiles.[4-11] The limitation with these systems is that, in the case of fatty acids, for example, increasing the carbon chain length from 15 to 16 transforms a liquidlike monolayer (hence readily accessible for examination by SLS) to a condensed monolayer which becomes difficult to probe by SLS.[10,11] Thus, in amphiphilic systems it is nearly impossible to develop a picture of the molecular properties which contribute to the monolayer viscoelasticity, based on a systematic variation in the chemical species. Only in the recent years have the dynamics of polymer monolayers been studied by means of SLS.[6,9,12-14]

This paper reports the dynamic results of a series of polymer monolayers in the order of increasing hydrophobicity poly(ethylene oxide), polytetrahydrofuran (PTHF), poly(vinyl acetate) (PVAc), poly(methyl acrylate) (PMA), poly(methyl methacrylate) (PMMA), and poly(*tert*-butyl methacrylate) (PtBMA). The first four form liquidlike monolayers which are ideally suited for SLS because of their intermediate elasticities. The last two, PMMA and PtBMA, form condensed monolayers which have large viscoelasticities making the analysis difficult. Nevertheless, they are still quite interesting in terms of monolayer phase behavior and dynamic surface tensions. Although all of these systems have similar static properties, by examining the dynamics we can indeed gain insight into the molecular origins of monolayer viscoelasticity.

Parenthetically, one should remark here that although PEO is referred as the least hydrophobic of the six polymers chosen, it is a special polymer in terms of its solubility in water as well as in a variety of organic solvents. Of polyoxides and polyethers, PEO and poly(vinyl methyl ether) are the only two that are soluble in water whereas poly(oxymethylene), poly(trimethylene oxide), poly(propylene oxide), PTHF, poly(butylene oxide), and poly(vinyl ethyl ether) are all water insoluble.[15] Hence, one must exercise caution in assigning a measure of hydrophobicity by means of a mean solubility parameter as we have done in Table I. Further, the surface activity of PEO in aqueous solution is also a novel feature[16] and its origin appears not very different from those of other water-insoluble polyethers and polyoxides, namely, due to amphiphilic character within a repeating unit composed of hydrophilic ether oxygen and hydrophobic oligomethylene linkage. In a very dilute solution of PEO in water, the

† Permanent address: Department of Industrial Chemistry, Faculty of Engineering, Mie University, Tsu, Mie 514, Japan.
‡ Present address: Central Research and Development Department, Experimental Station, E.I. du Pont de Nemours & Co., Wilmington, DE 19898.

0024-9297/89/2222-1735$01.50/0

Table I
Summary of Monolayer Parameters at 25 °C

polymer	A_0, m²/mg	$A_{0,m}$,[a] Å²/mon	δ,[b] (cal/cm³)$^{1/2}$	$\Gamma(\epsilon_{s,max})$,[c] ×10⁵ mg/cm²	$\Gamma(\epsilon_{max})$,[d] ×10⁵ mg/cm²	$\Gamma(\Delta f_{max})$,[e] ×10⁵ mg/cm²		$\Gamma(\kappa_{max})$,[f] ×10⁵ mg/cm²
						1	2	
PEO	4.16	30.4	17.7	4	4	4		
PTHF	2.90	34.7	16.5	5	5	3	10	
PVAc	1.73	24.7	15.8	9.5	9.5	5	16	11
PMA	1.67	23.8	16.0	9.0	9.0	5	13	10
PMMA	0.95	15.8	15.5	13		6		
PtBMA	1.14	26.9	14.6	10		8		10

[a] The limiting area per monomer unit, calculated from A_0. [b] The mean solubility parameters of a polymer segment on the water surface, taken from ref 23, are calculated by the geometric mean $(\delta_{water}\delta_{polymer})^{1/2}$ where δ_{water} and $\delta_{polymer}$ are the solubility parameters of water and polymer segment, respectively. [c] Surface concentration of each polymer when its static Gibbs elasticity, calculated according to eq 3, maximizes. [d] Surface concentration of each polymer when its longitudinal elasticity, calculated by the dispersion equation from the observed power spectra, maximizes (see Discussion in the text). [e] Surface concentration(s) of each polymer when its corrected spectral width $\Delta f_{s,c}$ reaches peak(s), where 1 and 2 stand for the Γ values of the first and second peaks in the cases of two peaks. [f] Surface concentration of each polymer when its longitudinal viscosity, calculated by the dispersion equation from the observed power spectra, maximizes (see Discussion in the text).

polymer is shown to adsorb spontaneously at the air/solution interface. It also forms a stable monolayer upon spreading it on the air/water interface as long as the surface concentration does not exceed a certain threshold; this point is further discussed in the Results.

Experimental Section

Materials. PEO with a molecular weight of $M_n = 144 \times 10^3$ g/mol and M_w/M_n less than 1.05 was from Toyo Soda Co. (supplied by Varian Associates, Sunnyvale, CA). PTHF was purchased from Polysciences (Warrington, PA). Its molecular weight was 130×10^3 g/mol and the polydispersity index was 1.15 according to the manufacturer. PVAc was polymerized by free radical polymerization and fractionated as reported previously.[12] Only one fraction with $M = 114 \times 10^3$ g/mol was used. PMA was prepared by solution polymerization of freshly distilled methyl acrylate in benzene at 70 °C for 2 h by using azobis(isobutyronitrile) (AIBN) as the initiator. The polymerized sample was precipitated by adding excess methanol and was dried under vacuum. The molecular weight of PMA was determined by intrinsic viscosity measurement in benzene at 30 °C from the relationship[17]

$$[\eta] = 4.5 \times 10^{-5} M^{0.78} \quad \mathrm{dL/g} \tag{1}$$

We used one PMA sample with the molecular weight of 589×10^3 g/mol.

Poly(methyl methacrylate) (PMMA) was prepared by bulk polymerization of purified monomer at 70 °C for 40 min with AIBN as an initiator in a Pyrex tube. The polymerized sample was dissolved in acetone and precipitated out in excess methanol. The precipitated sample was dried under vacuum and fractionated into 10 samples at 25 °C with acetone as the solvent and methanol as the nonsolvent. The molecular weights of fractionated samples were determined by intrinsic viscosity measurement in benzene at 25 °C from the relation[18]

$$[\eta] = 5.5 \times 10^{-5} M^{0.76} \quad \mathrm{dL/g} \tag{2}$$

The PMMA sample used had a molecular weight of 191×10^3 g/mol.

PtBMA was prepared by the ionic polymerization at low temperature. One PtBMA sample with the molecular weight of 140×10^3 g/mol and a molecular weight distribution of $M_w/M_n = 1.03$ was kindly provided to us by Dr. A. H. E. Müller of University of Mainz, Mainz, Germany.

The spreading solvent used to prepare polymer monolayers was spectrograde dichloromethane, and we used it without further purification.

Methods. All SLS experiments were performed simultaneously with the static surface tension measurements. A Teflon trough was filled with deionized water with the temperature controlled at 25 °C as was described previously.[11,12] Thirty minutes were allowed for the spreading solvent, dichloromethane, to evaporate completely. The surface pressure was measured by using a platinum plate connected to a Cahn 2000 electrobalance.

The SLS experimental setup has been described in detail elsewhere[19] and was designed after Hård et al.[20] The real image of a weak transmission grating, illuminated by a 7-mW He/Ne laser (Melles Griot), is focused by a series of two lenses on the liquid surface forming a real image on the surface 4 mm × 10 mm, and at the same time the diffraction spots are focused on the photocathode surface for heterodyne detection. The optics allow easy selection of different diffraction spots and thus different scattering angles ϕ, which is in turn related to the scattering wavevector k by $k = 2\pi \sin \phi \cos \theta/\lambda$, where $\theta = 64.4°$ is the incident angle measured from the normal to the surface and $\lambda = 632.8$ nm is the laser wavelength. We used four different wavevectors $k = 262$, 323, 385, and 445 cm^{-1} in this study.

The heterodyne power spectrum obtained on the spectrum analyzer (Nicolet 444A) is fitted to a Lorentzian function to obtain the peak frequency f_s, which is related to the propagation velocity of the capillary waves, and the full width at half-height Δf_s, which is related to the wave damping. The repeatabilities with independent sets of monolayers for f_s and Δf_s determinations were approximately within 0.5% and 5%, respectively. The corrected frequency width, $\Delta f_{s,c}$, is found by subtracting off the instrumental width Δf_i using $\Delta f_{s,c} = \Delta f_s - (\Delta f_i^2/\Delta f_s)$. The instrumental width is determined by measuring the full width at half-height of the intensity of the diffraction spot by scanning with a 20-μm pinhole.[20] All of the instrumental parameters used in this study have been summarized earlier.[21]

Before closing this Experimental Section, we should emphasize that although we have examined different molecular weight samples of PVAc[12] and PEO[13] and found them to be rather independent of M relative to their static properties, not all six polymers were equally subjected to the similar range of molecular weight. Hence we confine ourselves to one molecular weight sample each for the six polymers. With respect to the static surface pressure behaviors and longitudinal elasticities (see below), we can be quite certain that we are yet to find any molecular weight dependence, whereas the same cannot be said about the longitudinal viscosity μ since we have not yet performed a systematic examination. In this context, we start implicitly with an assumption that no sensitive molecular weight dependence is likely and we must search it carefully if there should be any to be found, and the assumption is in part justified from our results on PVAc[12] and PEO.[13]

Results

We now present the results of our study in the following order. First, we will show the static surface pressure profiles with respect to area per unit mass (Π–A) for four polymers and present how the two types of monolayers, the expanded and condensed, differ in the profiles. Next, we will present the spectral shift f_s and width $\Delta f_{s,c}$ profiles

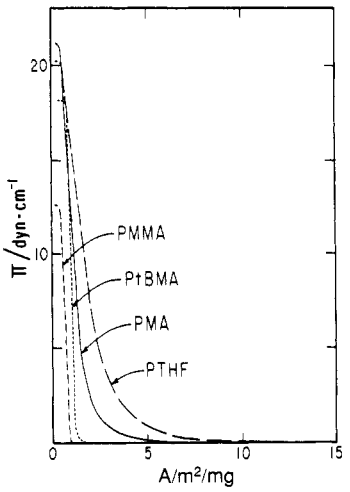

Figure 1. Surface pressure–area (Π–A) isotherms for four polymer monolayers at 25 °C.

with respect to the surface concentration Γ for all six polymers and distinguish them relative to the type of monolayers. For all three dependent variables, the qualitative features relative to A or Γ are delineated in this section. For more quantitative analyses of the deduced viscoelastic parameters, we will defer to the Discussion.

The surface pressure Π is plotted as a function of surface area per unit mass A(Π–A isotherm) for PTHF, PMA, PMMA, and PtBMA monolayers in Figure 1. PTHF and PMA monolayers are of the expanded type[1] where a finite value of Π is observed over a wide range of A. In general, Π gradually increases with decreasing A and finally shows a relatively steep increase before attaining a plateau value. This type of Π–A isotherm is similarly observed with PVAc and PEO monolayers, which have been reported in 1970 by Shuler and Zisman[16] and more recently from this laboratory in the context of SLS studies;[12,13] thus we did not include the data in Figure 1 to avoid repetition.

Since PEO is water soluble, a possibility of desorption from the surface must be addressed in terms of the stability of the monolayer.[13] In this context, we report that reversibility studies of the surface pressure for the all six polymers were performed whereby the monolayers were found to give reproducible values of the surface pressure upon repeating compression–expansion cycles as long as they were not compressed beyond a certain threshold, at which either film collapse or desorption is likely to take place. For PEO the threshold turned out to be about 9 dyn/cm, indicating that no PEO desorption from the surface into bulk solution was likely up to this value of Π, amounting to about 20 Å²/monomer unit.[13]

Contrary to those of PEO, PTHF, PVAc, and PMA, the Π–A isotherms for PMMA and PtBMA monolayers have sharper increases in Π as A decreases compared to the expanded monolayers. This is commonly ascribed to the presence of strong lateral interchain interactions. Starting at large areas, there is almost no increase in surface pressure until the abrupt increase in Π begins, whereby such a Π–A isotherm is referred to as a condensed isotherm. The limiting areas extrapolated to Π = 0 through the linear portion of the Π–A isotherms are smaller for these two polymers than those of expanded monolayers, and all are collected in Table I.

The frequency shifts f_s, a measure of the propagation velocity of the capillary waves, are plotted as a function of surface concentration Γ, which is the reciprocal A, in Figure 2 for different polymers at a wavenumber k = 323 cm⁻¹. The trend of the f_s versus Γ plot is seen to be universal within the range of observed k values; this is

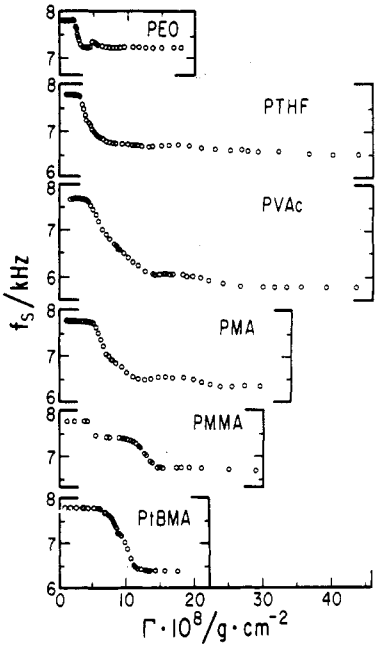

Figure 2. Plots of frequency shift f_s versus surface concentration Γ for six polymer monolayers at a scattering wavevector k = 323 cm⁻¹.

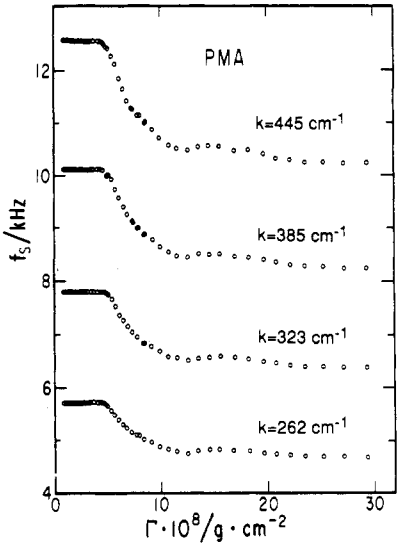

Figure 3. Plots of frequency shift f_s versus surface concentration Γ for PMA monolayers at four different scattering wavevectors as an example of expanded type.

shown in Figures 3 and 4, where typical plots of f_s versus Γ at four different k values for PMA and PMMA monolayers, respectively, as representative examples of each type of the monolayers, are displayed.

The next point to note about f_s–Γ plots for the expanded type monolayers is that prior to any decrease with increasing Γ, f_s is practically equal to that for the clean water surface. With increasing Γ, f_s decreases, essentially tracking the profile of surface tension with Γ, and then gradually reaches a constant value. There are small bumps in f_s for all four polymers after the initial decrease, and these bumps are interpreted in terms of the resonant coupling of the transverse and longitudinal waves as predicted by the dispersion equation (see below).

Turning to the condensed-type polymers, PMMA and PtBMA, the results in Figure 2 indicate that f_s decreases in a convex manner as the surface tension decreases before attaining a constant value. The profiles of f_s for PMMA also exhibit a distinctive feature which is absent from those

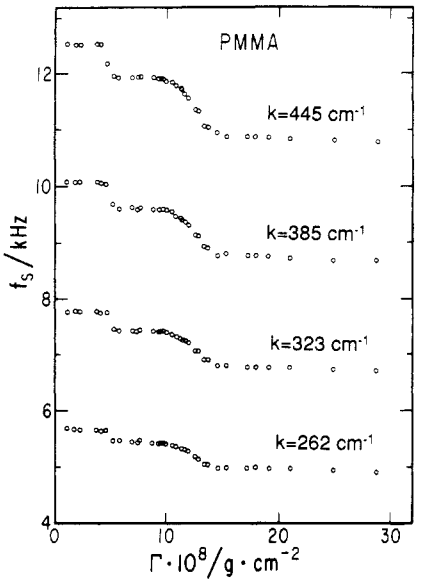

Figure 4. Plots of frequency shift f_s versus surface concentration Γ for PMMA monolayers at four different scattering wavevectors as an example of condensed type.

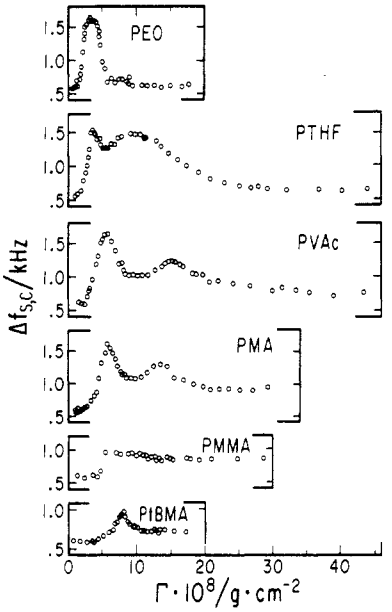

Figure 5. Plots of $\Delta f_{s,c}$ versus surface concentration Γ for six polymer monolayers at a scattering wavevector k = 323 cm^{-1}.

of the other five samples. At $\Gamma = 5 \times 10^{-5}$ mg/cm^2, f_s discontinuously drops by about 300 Hz. This is to be contrasted to the static surface pressure profile, which remains close to zero and shows no change until Γ exceeds 9.5×10^{-5} mg/cm^2. We attribute the precipitous drop to the onset of a biphasic state in PMMA. Some years ago, Crisp[1,2] was the first to report observing small but visible patches of condensed material with PMMA monolayers in the dilute region of surface concentration. We have similarly observed these patches starting at about $\Gamma = 5 \times 10^{-5}$ mg/cm^2, whereby the spectral width drop is ascribed to surface scattering from these patches, and the patches that are highly condensed hence have large values of elasticity, resulting in the drop of f_s.

The corrected width $\Delta f_{s,c}$ as a function of Γ for all six polymers at k = 323 cm^{-1} is presented in Figure 5 and the Γ values when $\Delta f_{s,c}$ maximize are also collected in Table I. The common trend in $\Delta f_{s,c}$ with respect to k with PTHF as an example is shown in Figure 6. The trend with k was observed for all others, but for brevity we do not show

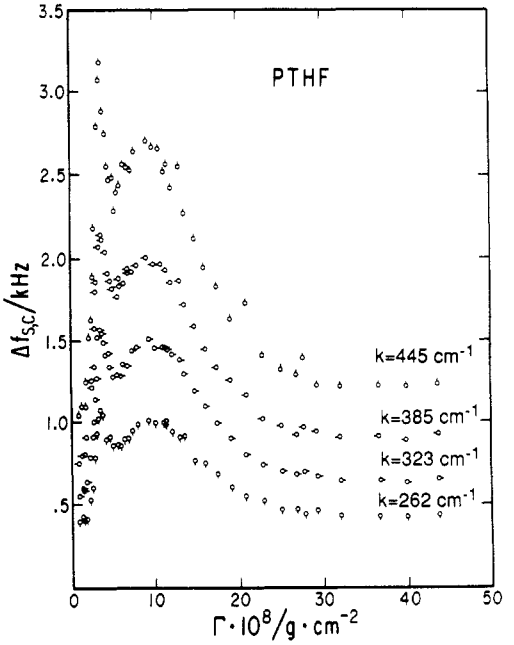

Figure 6. Plots of $\Delta f_{s,c}$ versus surface concentration Γ for PTHF monolayer at four different scattering wavevectors.

them here individually. With respect to the expanded-type monolayers, $\Delta f_{s,c}$ versus Γ of PEO has only one maximum while those of PTHF, PVAc, and PMA have two maxima (see Table I for a summary of these maxima). The magnitude of the first maximum is almost independent of polymer for the expanded-type monolayers including PEO, but the magnitude of the second peak at higher Γ depends sensitively on the nature of the polymer.

We now attempt to provide a qualitative but coherent picture of how the profiles of the four polymers appear differently. As discussed in the Introduction, the optimum resonant coupling between the capillary waves (controlled by the surface tension σ) and the longitudinal waves (controlled by $\epsilon^* = \epsilon - i\omega\kappa$, where $\omega = 2\pi f_s - i\pi\Delta f_{s,c}$) occurs[6-8] when the ratio of ϵ/σ reaches a value of about 0.2. If ϵ/σ exceeds 0.2 as Γ is increased, then the resonance condition is weakened whereby $\Delta f_{s,c}$ actually begins to decrease. As will be shown shortly, ϵ/σ increases with increasing Γ first and then decreases; the profiles of $\Delta f_{s,c}$ can be interpreted in terms of how ϵ/σ depends on Γ and whether ϵ/σ exceeds the threshold value of 0.2. For a given polymer, if the maximum value of ϵ/σ does not reach the threshold, the $\Delta f_{s,c}$ profile must have single maximum, whereas if it exceeds the threshold then the profile must have double maxima, with the second one equal or less in magnitude than the first depending on the κ variation with Γ. PEO belongs to the first case and all the other three belong to the second. This explains why PEO has only one peak in $\Delta f_{s,c}$; for PEO the elasticity does not reach above $\epsilon/\sigma = 0.2$ (or $\epsilon \approx 13$ dyn/cm).

The influence of κ on $\Delta f_{s,c}$ for the various polymers can also be estimated by looking at the raw spectral results. It is known theoretically[7] that an increase in κ is expected to decrease the maximum in $\Delta f_{s,c}$. Note that for PTHF in Figure 5 both maxima are almost the same magnitude indicating κ is relatively constant between the two maxima. The second peaks for PVAc and PMA are smaller than the first, indicating that κ is larger at Γ of the second maximum. All these ideas will be further supported in the next section where more quantitative values of ϵ and κ are obtained.

We now come to the two polymers, PMMA and PtBMA, which form the condensed-type monolayers. The values

of $\Delta f_{s,c}$ for the condensed monolayers are rather different from those of expanded-type monolayers. The results, however, are entirely understandable when examined in terms of monolayer viscoelasticity. In the plot of $\Delta f_{s,c}$ versus Γ for PtBMA monolayers (Figure 5), one clear maximum was observed at a surface concentration where the static surface pressure just begins to increase. The magnitude of the maximum in $\Delta f_{s,c}$, however, does not reach as high as those of the expanded-type monolayers because the elasticity becomes suddenly so large that the threshold condition, $\epsilon/\sigma = 0.2$, is difficult to capture experimentally. Once again the results for PMMA are qualitatively different than those for all the other polymers because of its biphasic nature in the dilute region. The values of $\Delta f_{s,c}$ for PMMA (Figure 5) show that at a concentration where the surface pressure is still almost zero, the damping coefficient undergoes a sharp increase and then gradually decreases with increasing concentration. The sharp increase in $\Delta f_{s,c}$ at $\Gamma = 5 \times 10^{-5}$ mg/cm^2 is again attributed to the scattering from the condensed patches of PMMA, similar to the case of an abrupt drop in f_s. It is interesting to note that similar changes in the spectra in the dilute region were seen for pentadecanoic acid,[11] PMMA,[14] a phospholipid,[21] and poly(vinyl stearate).[22]

These experimental results are summarized in Table I where A_0, the limiting area per unit mass, (with precision ±0.01), is contrasted to $A_{0,m}$, the limiting surface area per monomer unit (with precision ±0.4), by listing them side by side. Simultaneously, we indicate the progressive decrease of the geometric mean of solubility parameter relative to that of water, a measure of hydrophilicity.[23] In the last four columns, we list the observed surface concentrations when one of the dependent variables maximizes. Those values of Γ when ϵ and κ maximize will be taken up after the discussion of their profiles in the next section.

Discussion

Having provided a somewhat qualitative but coherent picture of how different profiles of Π, f_s, and $\Delta f_{s,c}$ should come about with respect to surface concentration, we now turn to more quantitative aspects of monolayer dynamics in terms of the longitudinal elasticity ϵ and the corresponding viscosity κ in conjunction with the static Gibbs elasticity ϵ_s. For the purpose of discussion, the polymers we have studied here will be grouped in three sets of two. In each set, the order of our discussion follows the sequence (1) evaluation of how ϵ, κ, and ϵ_s are determined, under what assumptions and with what precision; (2) comparison of ϵ and ϵ_s profiles with respect to Γ; (3) comparison of the profile of κ with respect to Γ; and (4) final brief remarks on comparison of the two.

We will start with the two polyethers. Although some of the results presented below have already appeared in print,[12,13] they are shown again here in order to make a direct comparison with the other polymers.

PEO and PTHF. A comparison of dynamic and static elasticities for PEO and PTHF is given in Figure 7A,C where ϵ_s was determined from the static Π–A isotherm via eq 3. The dynamic viscoelastic parameters ϵ and κ were

$$\epsilon_s = -A(\partial\Pi/\partial A) = \Gamma(\partial\Pi/\partial\Gamma) \qquad (3)$$

calculated with the dispersion equation[24,25] assuming $\sigma^* = \sigma_s$, which is equivalent to assuming $\mu = 0$ where the complex surface tension[6] is $\sigma^* = \sigma - i\omega\mu$ and μ is the transverse surface viscosity. Given the errors cited earlier in the Experimental Section for f_s, $\Delta f_{s,c}$, and Π, 0.5%, 5%, and 0.2 dyn/cm, respectively, the imprecision in calculation

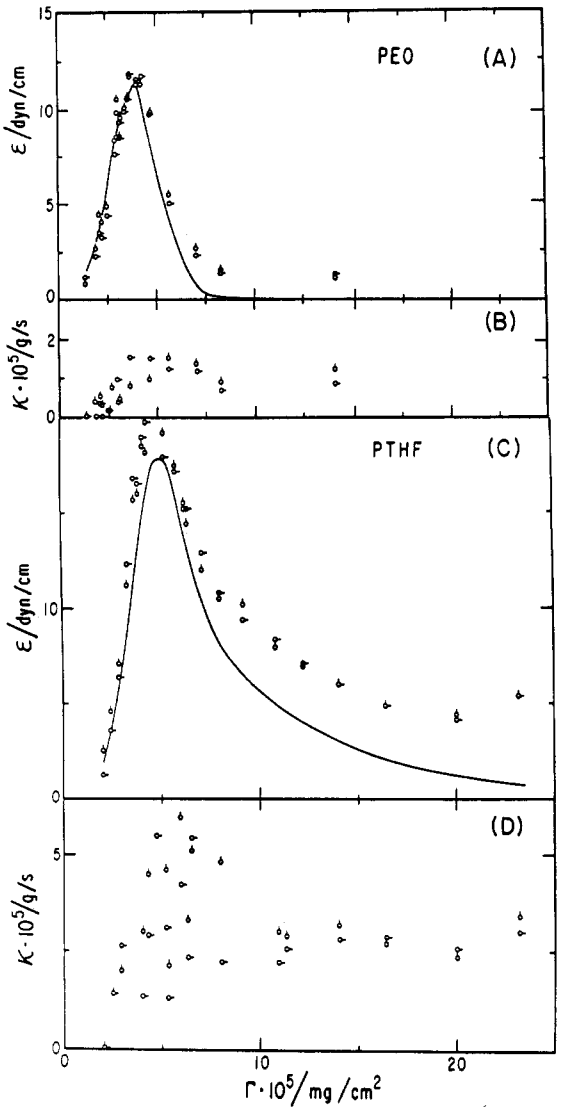

Figure 7. (A) Surface longitudinal elasticity versus surface concentration Γ for PEO. The static dilational elasticities are represented by the solid curve and the longitudinal elasticities at A/W obtained by SLS are represented at different values of k: $k = 323$ cm^{-1} (◇) and $k = 385$ cm^{-1} (○). (B) Surface longitudinal viscosity versus Γ for PEO. The results at different values of k are represented the same as in (A). (C) Surface longitudinal elasticity versus Γ for PTHF. The static dilational elasticities are represented by the solid curve and the dynamic longitudinal elasticities at different values of k are represented the same as in (A). (D) Surface longitudinal viscosity versus Γ for PTHF. The results at different values of k are represented the same as in (A).

of ϵ via the dispersion equation is about ±5% for PEO and 10% for PTHF. For κ the error is about ±30% for both PEO and PTHF. The reproducibility in κ at different concentrations can be estimated by examining the scatter in final values obtained at the two different k values as shown in Figure 7B,D.

The values of ϵ and ϵ_s for PEO come to a maximum at $\Gamma = 4 \times 10^{-5}$ mg/cm^2, while the maximum value for PTHF occurs at $\Gamma = 5 \times 10^{-5}$ mg/cm^2. PEO forms a less elastic monolayer with $\epsilon = 12.5$ dyn/cm at the maximum while PTHF has a maximum of about 20 dyn/cm. The dynamic and static elasticities are identical within experimental error at both values of $k = 323$ and 385 cm^{-1} until the surface concentration is past beyond that at the threshold. From that point on, the monolayer would presumably depart significantly from 2D conformations by chain looping, or possibly more macroscopic film collapse, so that the discrepancy between ϵ and ϵ_s is to be expected since

eq 3 no longer holds. The discrepancy is more prominent with PTHF and ϵ is about 5 dyn/cm while ϵ_s approaches zero at $\Gamma = 25 \times 10^{-5}$ mg/cm^2. For PEO the differences between ϵ and ϵ_s at the higher concentrations are less than 2 dyn/cm.

The corresponding surface longitudinal viscosity κ, which is a combination of compressional and shear components, was also calculated by using the dispersion equation. The values of κ in Figures 7B,D are zero at low concentrations and then begin to increase as ϵ increases and seem to reach a maximum at about the same point as ϵ. The values of κ for PTHF turned out to be about twice as large as those for PEO. There is only a small change in κ after the initial increase even when the monolayer is starting to collapse at approximately $\Gamma = 10 \times 10^{-5}$ mg/cm^2. The difference of the two must clearly be attributable to two additional methylene groups in PTHF, rendering it more hydrophobic thus engendering greater intersegmental interactions which result in larger magnitudes of ϵ and κ.

PVAc and PMA. The second set of polymers to be discussed form more condensed monolayers than the polyethers. At the outset, we should note that these two cannot be very different given their structural similarity. Given the errors in f_s, $\Delta f_{s,c}$, and Π of 0.5%, 5%, and 0.2 dyn/cm, respectively, the imprecision in calculation of ϵ via the dispersion equation, as the worst case estimate, is about ±15% for PVAc and ±10% for PMA. For κ the error is less than $\pm 2 \times 10^{-5}$ g/s for both PVAc and PMA at Γ less than 7×10^{-5} mg/cm^2 while above this concentration the error is between ±10% and ±50% with the higher errors mainly centered around the peak in elasticity.

The elasticities for PVAc and PMA maximize in Figure 8 at $\Gamma = 9.5 \times 10^{-5}$ mg/cm^2 and 9×10^{-5} mg/cm^2 with values of $\epsilon \approx 27.5$ dyn/cm and $\epsilon \approx 25$ dyn/cm, respectively. For PVAc the values of ϵ are a little more scattered around the peak but the departure of ϵ and ϵ_s seems to occur between $\Gamma = 10$ and 13×10^{-5} mg/cm^2 while for PMA the departure takes place between 13 and 14×10^{-5} mg/cm^2. The values of κ for these two polymers are also nearly identical at every concentration. For PVAc, κ remains between 0 and 1×10^{-5} g/s until $\Gamma = 5 \times 10^{-5}$ mg/cm^2, where it begins to increase substantially. The values of κ seem to maximize at the same concentration as ϵ and then begin to decrease before finally increasing to 28×10^{-5} g/s at $\Gamma = 23 \times 10^{-5}$ mg/cm^2. We are not sure why there is a maximum in κ at $\Gamma = 10$–12×10^{-5} mg/cm^2. On the other hand, it seems reasonable that the large increase at the highest concentrations comes about as the monolayer collapses and as the segments leave the interface there would be a large amount of segment–segment interaction. The values of κ for PMA remain below 2×10^{-5} g/s until $\Gamma = 7 \times 10^{-5}$ mg/cm^2 and then once again maximize at about the same concentration as ϵ does. After the maximum, κ decreases and then begins to increase at about $\Gamma = 15 \times 10^{-5}$ mg/cm^2 as the monolayer begins to collapse to a maximum of about 28×10^{-5} g/s at $\Gamma = 27 \times 10^{-5}$ mg/cm^2. The major difference between PVAc and PMA and the polyethers is that κ is much larger in magnitude and exhibits this interesting increase after the collapse of the monolayer for PVAc and PMA.

PMMA and PtBMA. The final comparison between PMMA and PtBMA in Figure 9 shows that both of these polymers form extremely viscoelastic monolayers. In this case ϵ and κ are imprecise because the capillary wave motion is insensitive to these parameters. The error bars on ϵ are one standard deviations among the three k vectors, 323, 385, and 445 cm^{-1}, and the error is large because of the large magnitude of ϵ. The values of ϵ for PMMA are zero until $\Gamma = 5 \times 10^{-5}$ mg/cm^2 and then ϵ jumps to 50–100 dyn/cm above this concentration. This is in direct contrast to ϵ_s (solid curve) which is zero until the increase at $\Gamma = 9.5 \times 10^{-5}$ mg/cm^2. The increase in ϵ at $\Gamma = 5 \times 10^{-5}$ mg/cm^2 is once again due to the biphasic nature of the monolayer in this dilute region. It seems to be a unique

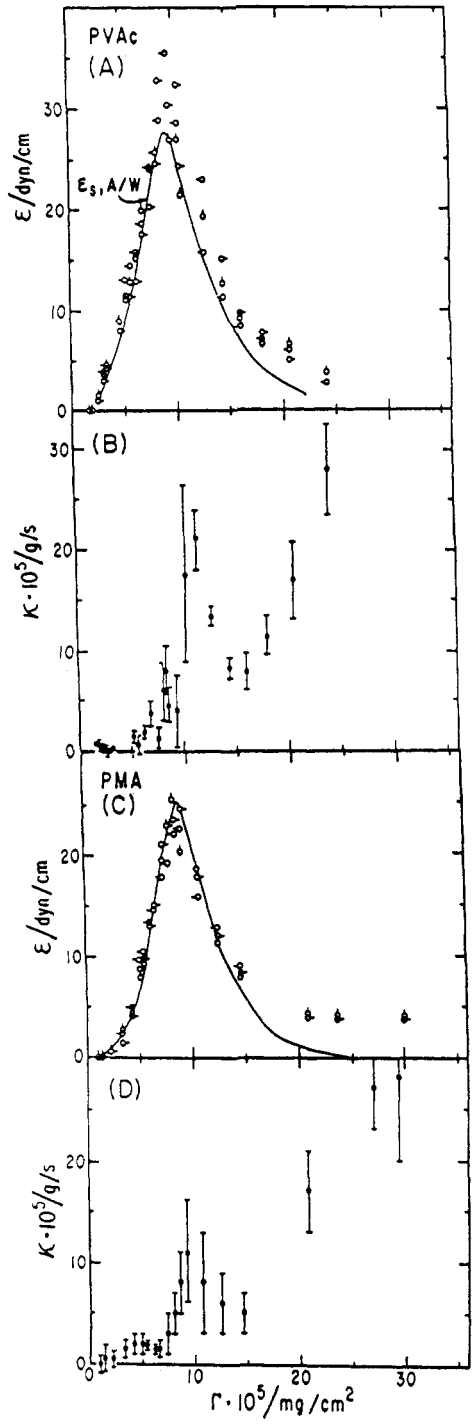

Figure 8. Surface longitudinal elasticity versus surface concentration Γ for PVAc. The static dilational elasticity is represented by the solid curve and the dynamic longitudinal elasticity is represented at different k values: $k = 323$ cm^{-1} (δ), $k = 385$ cm^{-1} (○), and $k = 445$ cm^{-1} (●). (B) Surface longitudinal viscosity versus Γ for PVAc. The bars represent standard deviation calculated from the variance between the three k values. (C) Surface longitudinal elasticity versus Γ for PMA. The static dilational elasticity is represented by the solid curve and the dynamic longitudinal elasticity is represented at different k values: same symbols as in (A). (D) Surface longitudinal viscosity versus Γ for PMA. The bars represent standard deviation calculated from the variance between the three k values.

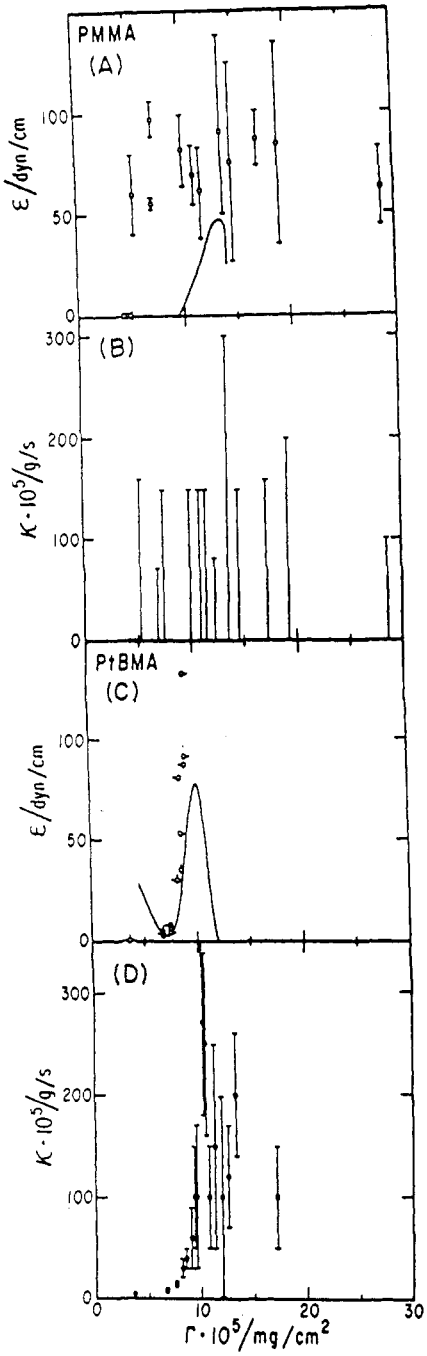

Figure 9. (A) Surface longitudinal elasticity ϵ versus surface concentration Γ for PMMA. The static dilational elasticity is represented by the solid curve. The error bars represent one standard deviation of ϵ for the three k values: 323, 385, and 445 cm^{-1}. (B) Surface longitudinal viscosity versus Γ for PMMA. The bars represent the range of possible values for κ at the three k values under the assumption that $0 < \Pi - \Pi_s < 1.5$ dyn/cm. (C) Surface longitudinal elasticity versus Γ for PtBMA. The static dilational elasticity is represented by the solid curve and the dynamic longitudinal elasticity is represented at different k values; $k = 323$ cm^{-1} (◇), $k = 385$ cm^{-1} (○), and $k = 445$ cm^{-1} (○). No values of ϵ are presented past $\Gamma = 9 \times 10^{-5}$ mg/cm^2. (D) Surface longitudinal viscosity versus Γ for PtBMA. The bars are one standard deviation for the calculated κ at the three κ values under the assumption that $\Pi = \Pi_s$.

characterization of this phase transition in the sense that we find the patches of condensed material to have very large values of ϵ and κ. In fact, these values are indistinguishable from the values in the uniphasic condensed region above 9.5×10^{-5} mg/cm^2.

The values of κ in Figure 9B follow the same trend as ϵ, starting at zero below $\Gamma = 5 \times 10^{-5}$ mg/cm^2 and increasing to around 100×10^{-5} g/s on the average at higher concentrations. These values should only be regarded as an estimate because the assumption that $0 < \Pi - \Pi_s < 1.5$ dyn/cm had to be made in orde to get nonnegative values of κ for most concentrations. This is why the bars which signify the upper limit of κ all start at zero.

PtBMA is quite different than PMMA in the sense that there is no biphasic region. The dynamic parameters were calculated by using the same assumption that was used for the expanded monolayers, i.e., $\Pi = \Pi_s$. The values of ϵ and ϵ_s eventually reach extremely large values in Figure 9C and they agree quite well from the dilute region up to about 50 dyn/cm. After $\Gamma = 9 \times 10^{-5}$ mg/cm^2, ϵ could no longer be calculated because of its large magnitude even though the static elasticity comes back down to zero after a sharp maximum at $\Gamma = 10 \times 10^{-5}$ mg/cm^2. This indicates that after the monolayer has collapsed ϵ is still too large to be determined precisely.

The values of κ in Figure 9D have a rather large error range as is indicated by the bars which are one standard deviations among the three k vectors. The values of κ seem to maximize at the same concentration as ϵ, but its significance is obscured by the large error range. What is important in a comparative sense is that the magnitude of κ is similar for PtBMA and PMMA and is significantly larger than those of the expanded monolayers.

We note here that a selected summary of the discussion we have developed so far is exhibited in Table I. We close this report by presenting a narrative summary of what we have learned.

Summary

The above are the individual summaries of the three sets of polymers, the two sets forming the expanded monolayers and the last set the condensed monolayers. We finally come to an overall summary. Selected values of κ are given in Table II at surface concentrations corresponding to $\epsilon_s = 6$ dyn/cm and also at $\epsilon_{s,max}$. Choice of $\epsilon_s = 6$ dyn/cm is entirely arbitrary, and we made it merely to compare all six polymers at a common value of ϵ_s. To estimate the relative contribution of ϵ and κ to the overall modulus ($\epsilon^* = \epsilon - i\omega\kappa$) we have also tabulated the viscosity contribution as the ratio of the viscous to elastic contributions via $2\pi f_s \kappa/\epsilon_s$ where f_s was taken at fifth-order diffraction corresponding to $k = 323$ cm^{-1} (see Figure 2 for approximate f_s values). The results at $\epsilon_s = 6$ dyn/cm indicate that κ for PTHF, PVAc, and PMA are about twice as large as that for PEO, while at $\epsilon_{s,max}$, values of κ for PVAc and PMA are about 10 times as large as those for PEO. At both ϵ and $\epsilon_{s,max}$ the ratio is less than 0.2 for PEO, PTHF, PVAc, and PMA while for PMMA and PtBMA the ratio is at least unity. The ratio for PMMA at $\epsilon_s = 6$ dyn/cm is 4.6 indicating that the viscous contribution is the dominant one. We should note here, however, that this can be misleading because $\epsilon_s \neq \epsilon$ for PMMA and the dynamic elasticity is actually much larger than the static value of $\epsilon_s = 6$ dyn/cm at that concentration (see Figure 9A), which would bring the ratio down to a more reasonable value.

In this section the inherent insensitivity of monolayer dynamics to the viscoelastic parameters ϵ and κ is used to our advantage by calculating dynamic surface tension. This serves two purposes: (1) the transverse surface viscosity can be determined, which is a rather controversial subject in the literature,[6,21] and (2) the experimental precision of our SLS results can be estimated by comparing Π and Π_s. By assuming some large value of ϵ and κ, say $\epsilon = 50$ dyn/cm and $\kappa = 1 \times 10^{-3}$ g/s, at all concentrations above $\Gamma = 5 \times 10^{-5}$ mg/cm^2 for PMMA and PtBMA, Π and μ were calculated for the wavevectors $k = 262$, 323,

Table II
Summary of Surface Viscosity Parameters of Six Polymers

	ϵ_s,[a] dyn/cm	κ, g/s	$2\pi f_s\kappa/\epsilon_s$[b]	$\epsilon_{s,max}$, dyn/cm	κ, g/s	$2\pi f_s\kappa/\epsilon_{s,max}$[b]
PEO	6	1 ± 0.5	0.08	12.5	1.5 ± 0.5	0.06
PTHF	6	2.5 ± 1	0.2	18	4 ± 2	0.1
PVAc	6	2 ± 1	0.16	27.5	15 ± 10	0.2
PMA	6	2 ± 0.5	0.16	25	10 ± 0.4	0.17
PMMA	6	60 ± 50	4.6	48	100 ± 70	1
PtBMA	6	15 ± 2	1.2	78	250 ± 70	1.4

[a] The value of ϵ_s = 6 dyn/cm was taken at the lower concentration side of the elasticity maximum. [b] Fifth-order diffraction values were used for f_s (see Figure 2).

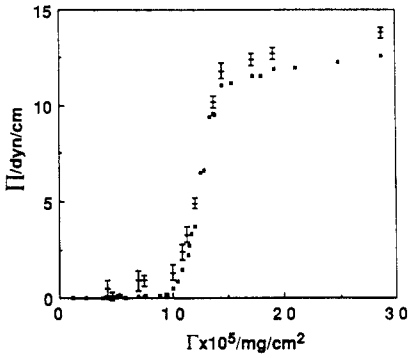

Figure 10. Static (squares) and dynamic (crosses with error bars) surface pressure versus surface concentration of PMMA. The error bars on the dynamic data points stand for one standard deviation of those values obtained at different scattering wavevectors k.

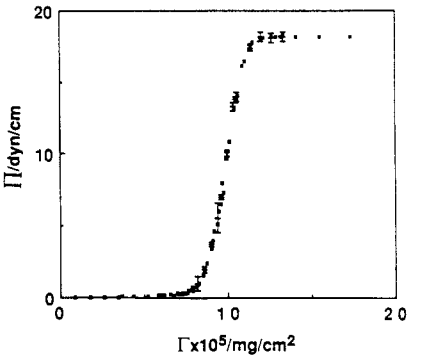

Figure 11. Static (squares) and dynamic (crosses with error bars) surface pressure versus surface concentration of PtBMA. The error bars on the dynamic data points stand for one standard deviation of those values obtained at different scattering wavevectors k.

385, and 445 cm^{-1}. These dynamic surface pressures are given for PMMA in Figure 10 where the error bars represent one standard deviation among those calculated at the four k values. The transverse surface viscosity was found to be $0 \pm 1 \times 10^{-5}$ g/s for all concentrations under these assumptions. The values of Π are consistently higher than Π_s at concentrations higher than 7×10^{-5} mg/cm^2, and these are shown in Figure 10. Of all the polymers we have thus examined, this is the singular case where Π and Π_s are distinctly different and here the difference amounts to only one dyn/cm. It is well-known that Π_s is quite time dependent upon compression of PMMA and since the dynamic measurements took substantially longer (about 20 min per concentration) than the static ones, it is quite plausible that $\Pi > \Pi_s$ if there were any conformational relaxation upon compression, since the relaxation should tend to give rise to lower apparent pressures if the films were overcompressed. The difference in the low concentration region between $\Gamma = 6$ and 9.5×10^{-5} mg/cm^2 where Π_s is essentially zero is probably due to the biphasic nature of the monolayer although further experiments in this dilute region are necessary to clarify this point.

Although PtBMA is similar in film viscoelasticity to PMMA, it is a better behaved system in many senses as is indicated in Figure 11 were Π and Π_s are identical within experimental error over the whole isotherm. The values of Π were calculated with the assumption that $\epsilon \geq \epsilon_s$ and $\kappa = 1 \times 10^{-3}$ g/s and the error bars in Figure 11 are one standard deviations as in PMMA case. There are no dynamic values below $\Gamma = 8.2 \times 10^{-5}$ mg/cm^2 because the large ϵ condition is no longer satisfied. Since there is no biphasic region here, Π and Π_s agree even in the lower surface concentration region. To estimate the effect of the assumption of $\epsilon \geq \epsilon_s$ on the calculation of Π, we tried by allowing ϵ to vary from the static value of $\epsilon_s = 75$ dyn/cm to infinity at a concentration of $\Gamma = 10 \times 10^{-5}$ mg/cm^2, for example, and examining how much Π changed. It turned out that Π varied only by 0.2 dyn/cm, hence the assumption is regarded as a critical element in calculating Π. Once again the transverse surface viscosity μ was found to be zero within experimental error in the range studied.

We conclude the paper with a brief summary of some of the more significant results. Although the elasticities of PEO and PTHF are quite similar, κ for PTHF is two to three times larger. PEO is very expanded on the surface and the low κ is probably due to a very low degree of cohesion. PVAc and PMA were almost identical relative to the magnitudes of ϵ and κ, which were slightly larger than those for PTHF. Since PMMA and PtBMA have the most significant viscous contribution to the dynamic modulus, we infer that this is due to the large segment–segment cohesion in the monolayer state while PEO has the smallest segment–segment cohesion. One last comparison deals with the collapse of the expanded monolayers which is monitored via ϵ and κ at high concentrations. PEO and PTHF are well above their bulk glass transition point at 25 °C, while PVAc and PMA are close to their glass transition point at this temperature. It is possible that this is why we see the large increase in κ after monolayer collapse for PVAc and PMA, while for the more liquidlike polyether monolayers κ does not change as the monolayer collapses.

Acknowledgment. This is in part supported by the Kodak Research Laboratories, the University Exploratory Research Program of the Procter and Gamble Co., and NATO Research Grant. We are most grateful to Dr. A. H. E. Müller of University of Mainz for the gift of PtBMA sample and fruitful discussion with our colleagues, Profs. George Zografi and Hyungsuk Pak and Dr. Kyung-Hwa Yoo. M.K. expresses his appreciation to the Yamada Foundation for travel support.

Note Added in Proof. In view of a most recent report by Vilanove et al.,[26] we append here our findings of the exponent y of $\Pi \propto \Gamma^y$, for the purposes of comparison, all at 25 °C for the six polymers examined together with the ranges of Π where y values have been determined.

polymer	y	Π, dyn/cm
PEO	2.77 ± 0.05	0.3–3.5
PTHF	2.2 ± 0.1	0.2–3
PVAc	2.80 ± 0.05	0.3–3
PMA	2.65 ± 0.10	0.2–12
PMMA	8.6 ± 1.0	0.2–10
PtBMA	13 ± 1	0.4–10

Registry No. PEO, 25322-68-3; PTHF (copolymer), 24979-97-3; PTHF (SRU), 25190-06-1; PVAC, 9003-20-7; PMA, 9003-21-8; PMMA, 9011-14-7; PtBMA, 25189-00-8.

References and Notes

(1) Crisp, D. J. *J. Colloid Sci.* **1946**, *1*, 49.
(2) Crisp, D. J. *J. Colloid Sci.* **1946**, *1*, 161.
(3) Dorrestein, R. *Proc. Kon. Ned. Akad. Wetensh., Ser. B. Phys. Sci.* **1951**, *54*, 260.
(4) Lucassen, J.; Hansen, R. S. *J. Colloid Interface Sci.* **1966**, *22*, 32.
(5) Lucassen, J.; Hansen, R. S. *J. Colloid Interface Sci.* **1967**, *23*, 319.
(6) Langevin, D. *J. Colloid Interface Sci.* **1981**, *80*, 412.
(7) Hård, S.; Löfgren, H. *J. Colloid Interface Sci.* **1977**, *60*, 529.
(8) Byrne, D.; Earnshaw, J. C. *J. Phys. D: Appl. Phys.* **1979**, *12*, 1145.
(9) Langevin, D.; Griesmar, C. *J. Phys. D: Appl. Phys.* **1980**, *13*, 1189.
(10) Hård, S.; Neuman, R. D. *J. Colloid Interface Sci.* **1981**, *83*, 315.
(11) Chen, Y.-L.; Sano, M.; Kawaguchi, M.; Yu, H.; Zografi, G. *Langmuir* **1986**, *2*, 349.
(12) Kawaguchi, M.; Sano, M.; Chen, Y.-L.; Zografi, G.; Yu, H. *Macromolecules* **1986**, *19*, 2606.
(13) Sauer, B. B.; Kawaguchi, M.; Yu, H. *Macromolecules* **1987**, *20*, 2732.
(14) Hård, S.; Neuman, R. D. *J. Colloid Interface Sci.* **1987**, *120*, 15.
(15) Molyneux, P. *Water-Soluble Synthetic Polymers: Properties and Behavior*; CRC Press: Boca Raton, FL, 1983; Vol. 1, Chapter 2.
(16) Shuler, R. L.; Zisman, W. A. *J. Phys. Chem.* **1970**, *74*, 1523.
(17) Krause, S. *Dilute Solution Properties of Acrylic and Methacrylic Polymers*; Rohm & Haas Co.: Philadelphia, PA, 1961; Part I, Revision I.
(18) Cantow, H.-J.; Schulz, G. V. *Z. Phys. Chem. (Frankfurt)* **1954**, *2*, 117.
(19) Sano, M.; Kawaguchi, M.; Chen, Y.-L.; Skarlupka, R. J.; Chang, T.; Zografi, G.; Yu, H. *Rev. Sci. Instrum.* **1986**, *57*, 1158.
(20) Hård, S.; Hamnerius, Y.; Nilsson, O. *J. Appl. Phys.* **1976**, *47*, 2433.
(21) Sauer, B. B.; Chen. Y.-L., Zografi, G.; Yu, H. *Langmuir* **1988**, *4*, 111.
(22) Chen, Y.-L.; Kawaguchi, M.; Yu, H.; Zografi, G. *Langmuir* **1987**, *3*, 31.
(23) Pak, H.; Kawaguchi, M.; Sano, M.; Yoo, K.-H.; Yu, H. Submitted for publication in *Macromolecules*.
(24) Lucassen-Reynders, E. H.; Lucassen, J. *Adv. Colloid Interface Sci.* **1969**, *2*, 347.
(25) Kramer, L. J. *J. Chem. Phys.* **1971**, *55*, 2097.
(26) Vilanove, R.; Poupinet, D.; Rondelez, F. *Macromolecules* **1988**, *21*, 2880.

The State of Hydrated Vanadyl Ions Adsorbed on a Perfluorinated Ionomer As Studied by ESR and ENDOR

Giacomo Martini,* M. Francesca Ottaviani, Luca Pedocchi, and Sandra Ristori

Department of Chemistry, University of Florence, 50121 Firenze, Italy.

Received August 8, 1988; Revised Manuscript Received October 12, 1988

ABSTRACT: An ESR and ENDOR study has been made of VO^{2+} water solutions at different metal ion concentrations adsorbed on the perfluorinated ionomer Nafion in its acidic form. The ESR parameters and the temperature dependence of the line shape indicated that the vanadyl probe maintained its square pyramidal structure and a relatively high mobility even at low temperatures. A very small fraction of these ions aggregated as dimers with an intercationic distance of ≥3.5–3.7 Å. The VO–F distance, as obtained from ENDOR experiments, confirmed that the ions were prevalently located in the ionic clusters that are formed after swelling with water. The ESR results were also discussed in terms of the polymer structure and of the properties of adsorbed water.

Introduction

Perfluorinated polymers consist of an organic backbone and ionic groups and are widely used as ionomeric materials. The presence of metal ions in these compounds has a profound relevance for the use in many processes and devices in several applications in the fields of electrochemistry and catalysis.[1-3] Ionomer membranes used for their ion selectivity or ion separation properties have been widely studied with different techniques to characterize either the effect of incorporated metal ions or their morphology both in the presence and in the absence of metal ions.[4-9] Most of the experimental techniques used for the study of perfluorinated ionomers suggest that their properties are very sensitive to the amount of adsorbed water and can be roughly explained on the basis of a phase separation into polar and nonpolar regions.[10] This results in an aggregation of the charges into the polar region. Several geometries have been suggested for the water-containing polymer, the most accepted being the so-called cluster-network model[11] in which approximately spherical holes (ionic clusters, whose diameter depends on the equivalent weight and on the water content) are connected through short and narrow channels.[12,13]

The electron spin resonance spectroscopy of transition-metal ions or of nitroxide radicals has been used to investigate both ionic mobility inside the ionic clusters and the peculiar behavior of the adsorbed water.[14-17] Recently we reported the use of neutral and charged nitroxides as sensitive probes toward the polarity changes of water adsorbed on the perfluorosulfonated membrane Nafion.[18] From the ESR line shapes of these radicals in the ionomer under conditions of full hydration and after exchange with different alkali and alkali-earth metal ions, we deduced that the ionic clusters have widely distributed sizes.

While the present work was in progress, an analysis of the ESR line-width behavior of aqueous solutions of vanadyl ions adsorbed on Nafion membrane was published.[19] The correlation times for the motion of the hydrated vanadyl ion are analyzed as a function of water content. Barklie et al. also give an estimation of the cluster sizes,

0024-9297/89/2222-1743$01.50/0